Optical bistability with symmetry breaking

AUTHOR(S):

Yabuzaki, T.; Okamoto, T.; Kitano, M.; Ogawa, T.

CITATION:

Yabuzaki, T. ...[et al]. Optical bistability with symmetry breaking. Physical Review A 1984, 29(4): 1964-1972

ISSUE DATE:

1984-04

URL:

http://hdl.handle.net/2433/152443

PHYSICAL REVIEW A VOLUME 29, NUMBER 4 APRIL 1984

Optical bistability with symmetry breaking

T. Yabuzaki, T. Okamoto, M. Kitano, and T. Ogawa
Radio Atmospheric Science Center, Kyoto University, Uji, Kyoto 611, Japan
(Received 25 October 1983)

It is shown that a simple system without a cavity exhibits optical bistability with no hysteresis but with symmetry-breaking or pitchfork bifurcation. The optical system is composed of a cell containing atoms with spin in the ground state, a $\lambda/8$ plate and a mirror, and an incident light beam linearly polarized and nearly resonant with the atomic absorption line. The system has a positive-feedback loop for the rotation of polarization through competitive optical pumping by $\sigma_{\pm}$ circularly polarized components. When the intensity of the incident light exceeds a critical value, symmetry breaking occurs and its polarization is subject to rotation in the clockwise or anticlockwise sense. Correspondingly, atomic spin polarization is produced spontaneously in a direction parallel or antiparallel to the incident beam. This new type of optical bistability is found to be explained well in context with the cusp catastrophe, as well as the ordinary one with hysteresis. It is also found that, in the presence of a transverse magnetic field, self-sustained spin precession occurs, which results in the steady-state modulation of the light polarization at about the Larmor frequency. Experimental evidence of the symmetry breaking and pitchfork bifurcation is obtained by using sodium vapor.

I. INTRODUCTION

In recent years optical bistability has attracted a great deal of attention, not only from the interests of its practical applications as an optical device but also from the theoretical interests of the phase transition in a nonequilibrium system.[1] Since the first demonstrative experiment of Gibbs *et al.*[2] in 1976, many optically bistable systems have been proposed and studied in detail theoretically and experimentally.[3] The optical bistability exhibited in all of these systems can be characterized by the presence of hysteresis, which appears in intensity changes of the output light (transmitted or reflected light) as the incident light intensity is varied.

The optical bistability that we propose and study in this paper is much different from ordinary bistability reported so far. The most striking difference is that this optical bistability has no hysteresis but has symmetry breaking (or a pitchfork bifurcation). The optical system has a positive feedback loop for the intensity difference of circularly polarized components of light, but not for the light intensity itself as in the ordinary optical bistable systems. When the incident light intensity exceeds a critical value and the differential gain overcomes the loss in the loop, the stable state bifurcates into two symmetrical branches and the system gets into either of these branches with equal probability. The jump between two stable branches, which can be observed in ordinary optical bistability, does not occur in the present system unless a circularly polarized light pulse is applied in addition. Analogous symmetry breaking or pitchfork bifurcation can be seen in an electronic flip-flop circuit (bistable multivibrator) when one increases gradually the dc voltage from zero and monitors the currents flowed in two transistors. So, the optical system that behaves with such a feature can be called an "optical flip-flop circuit." It must be noted that the symmetry breaking can be seen in optical tristability, which was proposed by Kitano *et al.*[4] and was quite recently observed experimentally by Cecchi *et al.*[5] by using a Fabry-Perot cavity filled with sodium vapor. In the case of optical tristability, the symmetry breaking occurs simultaneously with a jump in a doubled hysteresis cycle.

The optical system that will be studied theoretically and experimentally in this paper is very simple because it has no optical cavity. It consists of a cell containing atoms with spin in the ground state, which is used as a nonlinear dispersive medium, a $\lambda/8$ plate which polarizes the light elliptical, and a mirror to feed back the light to the cell. The incident light is near resonant to the atomic absorption line and linearly polarized. Competitive optical pumping by $\sigma_{\pm}$ components is caused by the optical feedback through the phenomenon called optically rotatory power,[6] or (optically induced) Faraday rotation. Two stable states of this system can be characterized by the polarization of output light or directions of spin polarization of atoms. In Sec. II we describe the setup of an optical system behaving with the new type optical bistability and study its stable states using a simplified three-level atomic model. The present optical bistability is discussed from the point of view of catastrophe,[7] and we show that it can be explained in context with the cusp catastrophe, similarly to the ordinary bistability with hysteresis.[8] In Sec. III we study theoretically the phenomenon of self-sustained spin precession occurring in this system when a static magnetic field is applied perpendicularly to the light beam. This results in the modulation of polarization of the output light at about the Larmor frequency. This phenomenon is similar to that in an optically tristable system, which was theoretically studied by Kitano *et al.*[9] and recently observed by Mitschke *et al.*[10] It is, however, basically different from the self-pulsing in an ordinary bistable system.[11] In Sec. IV we study experimentally the new type optical bistability, using sodium vapor and a laser beam tuned at the D_1 line, and we show an evidence of symmetry breaking and pitchfork bifurcation.

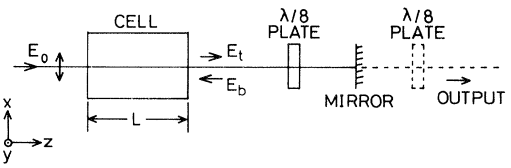

FIG. 1. Optical system exhibiting bistability with symmetry breaking, together with the definition of coordinates. The $\lambda/8$ plate shown by dashed lines is used to monitor the fields $\vec{E}_t$ and $\vec{E}_b$.

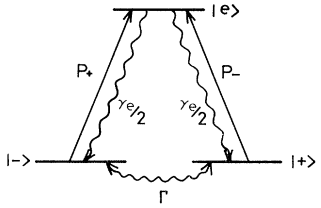

FIG. 2. Three-level atomic system with transitions by $\sigma_\pm$ circularly polarized light and relaxations.

II. OPTICAL SYSTEM AND STABLE STATES

The optical system consists of a cell containing atoms with Zeeman sublevels in the ground state, such as alkali-metal atoms, a $\lambda/8$ plate, and a mirror, as shown in Fig. 1. Incident light is linearly polarized and its frequency is near resonant to the atomic absorption line, i.e., it is in a region of anomalous dispersion. After being transmitted through the cell, the light is passed through a $\lambda/8$ and then reflected back to the cell by a mirror. Since the light beam passes the $\lambda/8$ plate twice, it plays the role of a $\lambda/4$ plate for a single path. So, unless the optical axis of the $\lambda/8$ plate is oriented to the direction parallel or perpendicular to the polarization of the incident light, the backward light is elliptically polarized in general, i.e., the intensities of $\sigma_\pm$ circularly polarized components become different. Because of this intensity difference, the atoms in the cell are optically pumped and atomic spins are oriented parallel or antiparallel to to the beam axis. When the spin polarization is produced in this way, the incident light is subjected to the rotation of polarization because of the difference of refractive indices for the $\sigma_\pm$ components. If the optical axis of the $\lambda/8$ plate is adequately oriented, the rotation of polarization for the incident light beam can increase the intensity difference of circularly polarized components in the backward light. As shown in Fig. 1, we take the x and z axis to the directions of polarization and propagation of the incident light, respectively. Let us write θ as the rotation angle of polarization and θ_0 as the angle between the x axis and the direction of optical axis of the $\lambda/8$ plate, which we shall call "offset angle."

A small amount of the light passed through the mirror is applied to another $\lambda/8$ plate shown by dashed lines in Fig. 1, which is used to monitor the changes of polarization and intensities of the forward- and backward-light beams. When the optical axes of two $\lambda/8$ plates are oriented perpendicularly to each other, the phase retardation is canceled out so that the polarization of the output light becomes the same as that of the forward-light beam transmitted through the cell. On the other hand, when they are oriented parallel to each other, the polarization of the output light becomes the same as that of the backward light fed back to the cell.

Let us consider the three-level atomic system, where two levels are the spin-up and spin-down levels in the ground state, and the other is a representative excited state (see Fig. 2). The ground-state sublevels are degenerate and have equal number densities $N_+=N_-=N_0/2$ in the absence of light beams, where N_0 is the total number density. The decay rate γ_e of the optically excited state $|e\rangle$ is, in general, much larger than the spin-relaxation rate Γ, and the transitions from $|e\rangle$ to $|\pm\rangle$ are assumed to have equal probability. In such a three-level system, the effect of optical pumping can be described by the rate equation as

$$\frac{dN_\pm}{dt}=-P_-N_++P_+N_--\frac{\Gamma}{2}(N_\pm-N_\mp)\,, \tag{1}$$

where the population in the $|e\rangle$ state has been neglected by assuming that the pumping rates $P_\pm$ for the $\sigma_\pm$ light are much smaller than the decay rate γ_e. The pumping rates $P_\pm$ are proportional to the intensities (photon flux) $i_\pm$ of $\sigma_\pm$ components,

$$P_\pm=\tfrac{1}{2}\sigma i_\pm\,. \tag{2}$$

For a homogeneously broadened medium as in the present experiment described later, the absorption cross section σ for the monochromatic light with frequency ω is given by

$$\sigma=\frac{4\pi d^2\omega_0}{c\hbar}\frac{\gamma_c}{(\Delta\omega)^2+\gamma_c^2}\,, \tag{3}$$

where d is the dipole moment, γ_c is the relaxation rate for coherence between the ground state and the excited state, ω_0 is the transition frequency, and $\Delta\omega=\omega_0-\omega$. The steady-state solutions of Eq. (1) can be easily obtained as

$$N_\pm=\frac{I_\pm+1}{I_++I_-+2}N_0\,, \tag{4}$$

where $I_\pm$ are the normalized light intensities defined as

$$I_\pm=(\sigma/\Gamma)i_\pm\,. \tag{5}$$

Let us hereafter express the light intensity by its normalized form as above. The wave numbers $k_\pm$ and the absorption coefficients $\alpha_\pm$ for $\sigma_\pm$ components can be expressed in terms of the number densities $N_\pm$ as

$$k_\pm=k_0+(\sigma/2)(\Delta\omega/\gamma_c)N_\mp\,, \tag{6}$$

$$\alpha_\pm=(\sigma/2)N_\mp\,, \tag{7}$$

where k_0 is the wave number in a vacuum. For simplicity, we will hereafter neglect the absorption losses $\alpha_\pm$ by taking a relatively large value of $|\Delta\omega|$. In our experiment to be described in Sec. IV, the value of $|\Delta\omega|/\gamma_c$ is chosen to be about 10. In such a case, the absorption losses were found not to cause significant effects from the

numerical calculations. The angle θ of polarization rotation for the linearly polarized component can be written as

$$\theta=(-L/2)(k_+-k_-)$$
$$=kL\frac{I_+-I_-}{I_++I_-+2}\ , \tag{8}$$

where k is the value of $k_\pm-k_0$ in the case that no optical pumping takes place, i.e.,

$$k=\frac{\sigma}{2}\frac{\Delta\omega}{\gamma_c}\frac{N_0}{2}\ . \tag{9}$$

If we express the atomic system in terms of macroscopic magnetization instead of number densities $N_\pm$, the equation of motion (1) can be rewritten as

$$\frac{dm_z}{dt}=-\Gamma(1+I_0)m_z+\Gamma\sin(2kLm_z)\ , \tag{10}$$

where m_z is the z component of magnetization normalized by the maximum value M_0 $(=1)$. In this case, the rotation angle θ can be expressed in terms of the macroscopic magnetization as

$$\theta=kLm_z\ . \tag{11}$$

When the incident light is subjected to the rotation of polarization, the electric field after being transmitted through the cell can be written as

$$\vec{\mathrm{E}}_t=(\vec{e}_x\sin\theta+\vec{e}_y\cos\theta)E_0\ , \tag{12}$$

where E_0 is the electric field intensity of the incident light beam, i.e., $(\sigma/T)E_0^2=I_0$, and $\vec{e}_x$ and $\vec{e}_y$ are unit vectors representing the x and y directions. After it is passed twice through the $\lambda/8$ plate, the electric field of the backward light becomes

$$\vec{\mathrm{E}}_b=\vec{\mathrm{E}}_{b+}+\vec{\mathrm{E}}_{b-}\ , \tag{13}$$

where $\vec{\mathrm{E}}_{b\pm}$ represent the $\sigma_\pm$ components in the backward-light beam, which are given by

$$\vec{\mathrm{E}}_{b\pm}=(E_0/4)[\sin(\theta+\theta_0)+\cos(\theta+\theta_0)](\vec{e}_x\pm i\vec{e}_y)\ . \tag{14}$$

Since atoms move many wavelengths during the pumping time, the effect of the standing-wave structure of the field is expected to be smeared out. As a result, the light intensity effective to the optical pumping is given by the sum of intensities of forward and backward beams. Thus, the total intensities of circularly polarized components within the cell becomes

$$I_\pm=I_0\{1\pm\tfrac{1}{2}\sin[2(\theta+\theta_0)]\}\ . \tag{15}$$

The intensity difference I_+-I_- produces the spin polarization, which causes the rotation of polarization for the forward-light beam. Inserting (15) into (8), we obtain the equilibrium rotation angle θ as

$$\theta=\frac{kL}{2}\frac{I_0\sin2(\theta+\theta_0)}{I_0+1}\ . \tag{16}$$

Similar expression for the steady-state magnetization m_z is obtained by inserting (16) into (11).

From Eq. (16) one may immediately find that the system has bistable or multistable states when kL and I_0 satisfy the conditions as

$$kL>1,\quad I_0>I_{\mathrm{cr}}\ , \tag{17}$$

where the critical intensity I_{cr} is given by

$$I_{\mathrm{cr}}=1/(kL-1)\ . \tag{18}$$

Figure 3(a) shows the equilibrium values of θ as a function of incident light intensity I_0 in the case that $\theta_0=0$. The stable and unstable values are shown by solid and dotted lines, respectively. When I_0 is increased from zero and exceeds the critical value given by (18), a symmetry breaking takes place and the rotation of polarization occurs toward either the positive or negative direction with equal probability. The upper and lower branches in Fig. 2(a) correspond to the atomic stable states in which spins in the ground state are oriented parallel and antiparallel to the light axis. The stable and unstable states with $\theta=0$ correspond to the random spin polarization. Such a change of the system may be called "pitchfork bifurcation." It is important to note that a hysteresis cycle cannot be seen in the rotation angle θ as a function of I_0. Figure 3(b) shows the cases that the offset angle θ_0 is 7°, 12°, and 18°. When θ_0 has nonzero value, θ changes monotonously as seen in Fig. 3(b) because the amplification of θ becomes asymmetrical for the directions of rotation

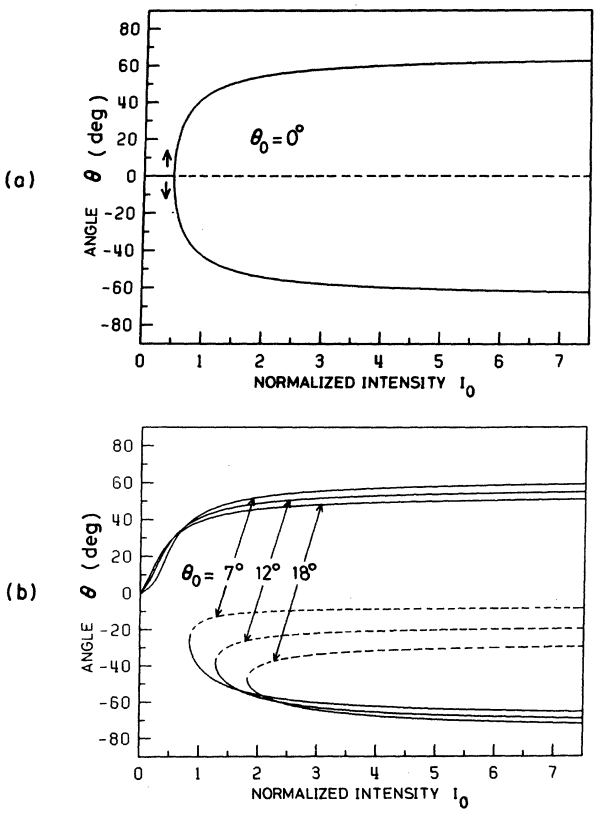

FIG. 3. Equilibrium rotation angle θ as a function of incident light intensity I_0 in the case where (a) $\theta_0=0$, and (b) $\theta_0=7°$, 12°, and 18°. In above cases kL is fixed at 3. Dashed lines show the unstable equilibrium values.

of polarization. Even in these cases, there appears another stable state when I_0 exceeds a critical value, but the system does not get into this state unless it is subjected to additional perturbation to convert the direction of spin polarization.

The switching between stable states in the bistable region becomes possible by applying an additional pulsed circularly polarized light, if it is strong enough to reverse the direction of spin polarization produced by the cw light. Let us write $I(t)$ as the normalized intensity of the pulsed light. Under the action of such a pulsed light beam in the case of $\theta_0=0$, the equation of motion for the z component of the magnetization m_z can be obtained by replacing I_0 in Eq. (10) by I_0+I_t:

$$\frac{dm_z}{dt}=-\Gamma\left[1+I_0+\frac{I(t)}{2}\right]m_z + \frac{\Gamma I_0}{2}\sin[2kLm_z+I(t)] \ . \tag{19}$$

By solving Eq. (19) and inserting the solution into Eq. (11), the change of the rotation angle θ can be obtained. Figure 4 shows the change of θ by a square pulse with the normalized height 3 and duration 5×10^{-5} s in the case that $kL=3$, $I_0=5$, and $\Gamma=1000$/s. In this way we see that a pulsed circularly polarized light can be used for the switching between stable states, just as a pulsed signal in a flip-flop circuit.

It is interesting to discuss the present optical bistability from the point of view of catastrophe.[7] We would like to show here that the present bistability can be explained in context with the cusp catastrophe, with which ordinary optical bistability with hysteresis was also explained well by Agrawall and Carmichael.[8] The system potential for the cusp catastrophe is expressed in a form as

$$V(x)=\tfrac{1}{4}x^4+\tfrac{1}{2}ux^2+vx \ , \tag{20}$$

where x is the behavior variable, and u and v are the control parameters. The steady-state surface (x,u,v) can be obtained by setting $\partial V(x)/\partial x=0$ in (20), i.e., from $x^3+ux+v=0$. One might easily find that, when u is set constant to an adequate value, $x(v)$ in equilibrium shows an S-shaped curve (or a hysteresis curve in steady state) as seen in the ordinary optical bistability. So, for the ordinary optical bistability, the behavior variable x and control parameter v can be linearly related with intensities of output and incident light, respectively. On the other hand, when v is fixed at zero and u is varied, $x(u)$ exhibits a pitchfork bifurcation with symmetry breaking occurring at $u=0$. Among three equilibrium branches in the region $v\geq0$, the branch $x(u)=0$ is unstable. Thus, we obtain the similarity with the present bistability, relating x to the rotation angle θ (or magnetization m_z) and u to the incident light intensity I_0. Then, one might have the question of what quantity relates to u and gives a hysteresis cycle in the rotation angle θ when the value is varied? From Eq. (16) one might see that the quantity is the offset angle θ_0 of the optical axis of the $\lambda/8$ plate. Figure 5 shows the calculated rotation angle θ as a function of θ_0, in which I_0 is varied as a parameter. In Fig. 5, we see that the surface representing (θ,I_0,θ_0) is quite resemblant to the steady-state surface of the cusp catastrophe.[7] In this way, we see that the present optical bistability belongs to the same catastrophe as the ordinary one, and different features can be explained by orthogonal cross sections of the steady-state surface.

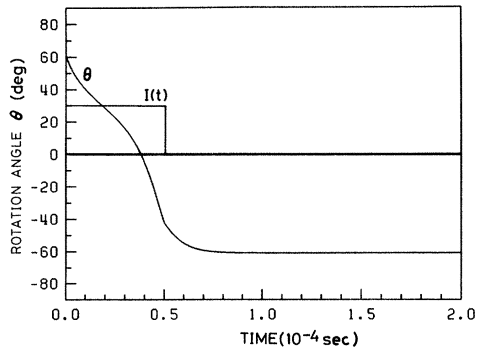

FIG. 4. Change of the rotation angle θ by a circularly polarized pulse in the case that $kL=3$ and $I_0=5$. The square pulse has normalized intensity 3 and duration 5×10^{-5} s. The spin relaxation rate Γ is set at 1000/s.

III. SELF-PULSING BY SPIN PRECESSION

Let us consider the case where a static magnetic field $\vec{H}_0$ is applied transversely to the laser beam in Fig. 1. In the transverse magnetic field $\vec{H}_0$, the Bloch equation for the normalized magnetization m can be written in the form

$$\frac{d\vec{m}}{dt}=\gamma\vec{m}\times\vec{H}_0-\Gamma\vec{m}-P_+(\vec{m}-\vec{m}_0)-P_-(\vec{m}+\vec{m}_0) \ , \tag{21}$$

where γ is the gyromagnetic ratio, $\vec{m}_0$ is the maximum magnetization ($|\vec{m}_0|=1$) along the direction of the incident beam, i.e., the z direction. When the y axis is taken to the direction of $\vec{H}_0$, the equations of motion for the x and z components of $\vec{m}$ become

$$\frac{dm_x}{dt}=-\Omega_0m_z-\Gamma\left[1-\frac{(I_++I_-)}{2}\right]m_x \ , \tag{22}$$

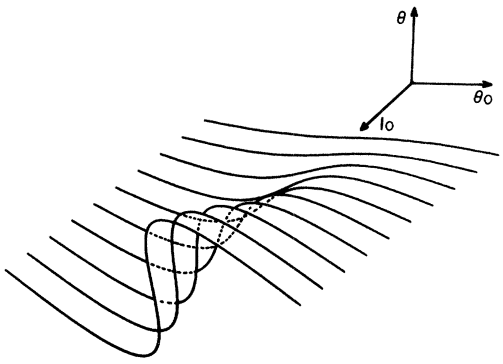

FIG. 5. Rotation angle θ as a function of the offset angle θ_0. The incident light intensity I_0 is varied as a parameter.

$$\frac{dm_z}{dt}=\Omega_0 m_x-\Gamma\left[1+\frac{(I_++I_-)}{2}\right]m_z$$
$$+\Gamma\frac{(I_+-I_-)}{2}\sin(2kLm_z)\ , \tag{23}$$

where Ω_0 is the Larmore frequency, i.e., $\Omega_0=\gamma H_0$. It is unnecessary to consider the y component of $\vec{m}$, because it does not couple to $m_{x,z}$ and decay exponentially to zero.

Let us consider a particular case where $\theta_0=0$. By using Eqs. (8) and (11), Eqs. (22) and (23) can be rewritten in this case as

$$\frac{dm_x}{dt}=-\Omega_0 m_z-\Gamma(1+I_0)m_x\ , \tag{24}$$

$$\frac{dm_z}{dt}=\Omega_0 m_x-\Gamma(1+I_0)m_z\frac{\Gamma I_0}{2}\sin(2kLm_z)\ , \tag{25}$$

where we have replaced I_++I_- in Eqs. (22) and (23) by $2I_0$, assuming that the light absorption is negligibly small. Eliminating m_x from Eqs. (22) and (23), we obtain the equation of motion for m_z as

$$\frac{d^2m_z}{dt^2}+f(m_z)\frac{dm_z}{dt}+g(m_z)=0\ , \tag{26}$$

with

$$f(m_z)=\Gamma[2+2I_0-kLI_0\cos(2kLm_z)]\ , \tag{27}$$

$$g(m_z)=\Omega_0^2 m_z+\Gamma^2(1+I_0)^2m_z$$
$$-(\Gamma^2/2)I_0(I_0+1)\sin(2kLm_z)\ . \tag{28}$$

When $\sin(2kLm_z)$ is expanded with respect to m_z up to the second order, Eq. (26) becomes exactly the van der Pol equation that describes the behavior of an electron tube oscillator.[12] Thus we can expect that $\vec{m}$ precesses around $\vec{H}_0$ without any external driving force, such as the rf magnetic field to induce the magnetic resonance.

The stability of magnetization $\vec{m}$ under the presence of the magnetic field $\vec{H}_0$ can be studied by using the asymptotic or phase-plane method,[13] and one might easily find that different types of the steady-state solutions of Eqs. (24) and (25), or Eq. (26), are obtained in three regions of the incident light intensity I_0. The stable magnetization vector $(m_x,m_z)_s$ in three regions becomes as follows, under the condition that its absolute value is not large $[\cos(2kLM_z)\simeq 1]$.

(i) In the region $I_0\le(kL-1)^{-1}$,

$$(m_x,m_z)_s=(0,0) \tag{29}$$

for any value of Ω_0.

(ii) In the region $(kL-1)^{-1}<I_0<2(kL-2)^{-1}$,

$$(m_x,m_z)_s\begin{cases}(0,0), & \Omega_0\ge\Omega_{\rm cr} \quad (30)\\ (\mu,\nu), & \Omega_0<\Omega_{\rm cr}\ , \quad (31)\end{cases}$$

where μ and ν represent nonzero numbers, and the critical value $\Omega_{\rm cr}$ of Larmor frequency is given by

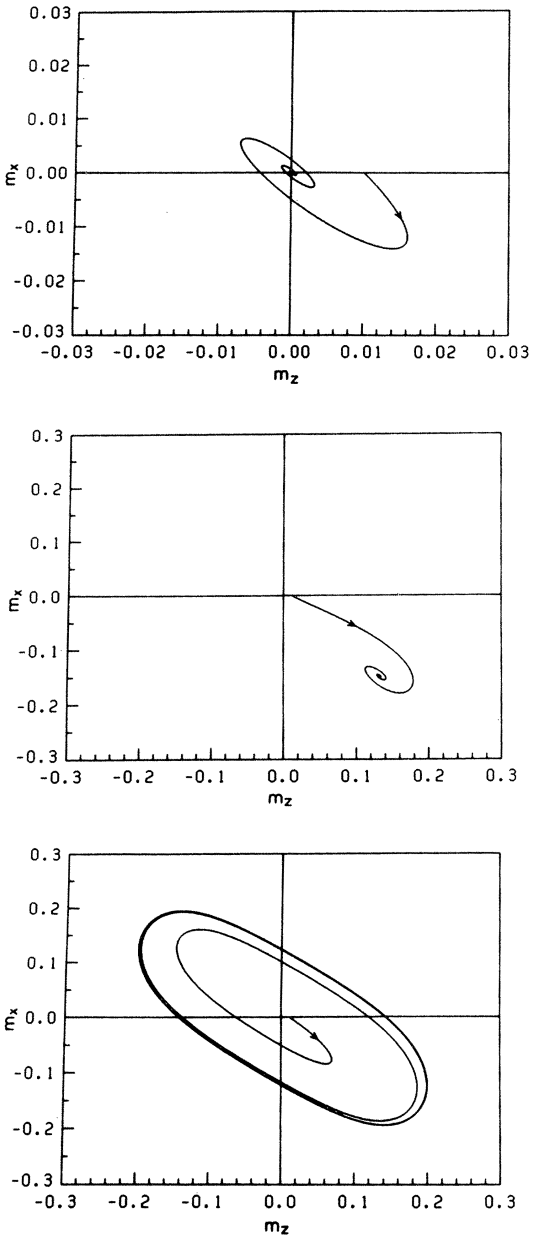

FIG. 6. Trajectories of normalized magnetization $\vec{m}$ on a plane perpendicular to the static magnetic field $\vec{H}_0$, in the cases where (a) $I_0=1.0$, $\Omega_0=20$, (b) $I_0=3.0$, $\Omega_0=45$, and (c) $I_0=3.0$, $\Omega_0=55$. In the above cases, kL is fixed at 3.5.

$$\Omega_{\rm cr}=\Gamma[(I_0+1)(kLI_0-I_0-1)]^{1/2}\ . \tag{32}$$

(iii) In the region $I_0\ge 2(kL-2)^{-1}$,

$$(m_x,m_z)_s=(\mu,\nu),\quad \Omega_0<\Omega_{\rm cr}\ , \tag{33}$$

$$\{(m_x,m_z)_s\}\rightarrow\mathscr{C}_{m_x,m_z},\quad \Omega_0\ge\Omega_{cr}\ , \tag{34}$$

where $\mathscr{C}_{m_x,m_z}$ is a limit cycle in the m_x-m_z plane, enclosing the origin (0,0).

Figure 6 shows the trajectories of $\vec{m}$ calculated numeri-

cally by using Eqs. (24) and (25); in Fig. 6(a), $kL=3.5$, $I_0=1.0$, $\Omega_0=20$; in Fig. 6(b), $kL=3.5$, $I_0=3.0$, $\Omega_0=45$; and in Fig. 6(c), $kL=3.5$, $I_0=3.0$, $\Omega_0=55$, for which the steady-state solutions are given by (30), (33), and (34), respectively. As seen in Fig. 6(c), the magnetization, starting from the nearly zero value, spirals out and approaches asymptotically a limit cycle. It must be noted that when θ_0 is not zero, the growth of m_z is much faster than the above case of $\theta_0=0$, and the limit cycle becomes asymmetric with respect to the origin $m_z=(0,0)$. The frequency of the spin precession is lower than the Larmor frequency Ω_0. Figure 7 shows the numerically calculated precession frequency as a function of Ω_0, in the cases that $\theta_0=0$, $kL=3.5$, and $I_0=3.0$, 6.0, and 9.0. As seen in Fig. 7, the precession frequency at the critical value of Ω_0 is considerably lower than the Larmor frequency (the straight line from the origin), and it approaches asymptotically to Ω_0 with the increase of the applied field intensity. It must be noted that the critical value of Ω_0 is lower than Ω_{cr} given by Eq. (32), the deviation being larger for the larger value of I_0. This is because Eq. (32) holds only when the absolute value of magnetization is not so large. The self-sustained spin precession can be observed as the modulation of the rotation angle θ for the forward-light beam or as the alternative switching of $\sigma_{\pm}$ components in the backward beam. The upper limit of the precession frequency may be roughly given by the width of the absorption line.

IV. AN EXPERIMENT WITH SODIUM VAPOR

An experiment to realize the new type optical bistability has been carried out by using the optical system schematically shown in Fig. 8, in which a $\lambda/4$ plate is used instead of the $\lambda/8$ plate. The light from a cw dye laser, tuned on a wing of the Na-D_1 line, is applied to the sodium cell (heat pipe oven) with 25-cm length and 1.6-cm i.d. The

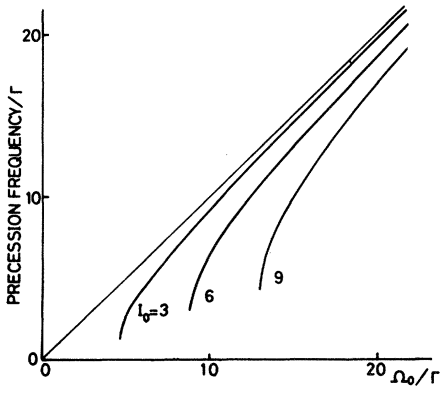

FIG. 7. Frequency of the steady-state precession of $\vec{m}$ as a function of the strength of the applied magnetic field in terms of Ω_0 for three values of I_0. The straight line from the origin shows the frequency of free precession.

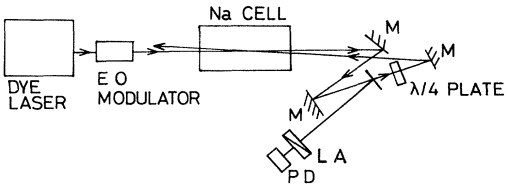

FIG. 8. Schematic illustration of experimental setup. Symbols have the following significance: M, mirror; LA, linear analyzer; and PD, photodetector.

cell contains helium gas at about 500 torr, at which the pressure broadening of the D_1 line by the helium gas was measured to be about 8 GHz [half-width at half maximum (HWHM)]. This value is much larger than the Doppler width ($\sim$1.7 GHz) and the hyperfine splitting in the ground state of sodium (1.7 GHz). Therefore, we can neglect the hyperfine optical pumping. In addition, the excited state $3\,^2P_{1/2}$ is completely mixed at this helium pressure, so that the three-level approximation used in Sec. II may be good under the present condition. After it passes through the cell, the light beam is transmitted through a $\lambda/4$ plate and then fed back to the cell. The $\lambda/4$ plate for a single optical path is equivalent to the $\lambda/8$ plate in the optical system shown in Fig. 1. The incident light intensity I_0 is varied in the range 0—120 mW by using an electro-optic modulater. The beam diameters of the incident and backward beams were, respectively, 5 and 8 mm at the position of the sodium cell. A beam splitter is inserted between the cell and the $\lambda/4$ plate, and the rotation of polarization θ is measured by detecting the intensity of the light passed through a linear analyzer whose optical axis is inclined by 45° from the polarization axis of the incident light. Thus, the detected light intensity I_d is given by $I_0\cos^2(\theta+\pi/8)$, when the absorption of the light can be neglected. The detuning $\Delta\omega$ of the laser frequency from the center of the D_1 was measured by applying a part of laser output to a Na cell without a buffer gas and to a Fabry-Perot interferometer. In the present experiment, the detuning $\Delta\omega$ was kept constant at 100 GHz, and the cell temperature at 463 K, which gives the sodium density of $\sim 2.3\times 10^{12}$ cm^{-3}.

Figure 9 shows the experimentally obtained change of the detected light intensity I_d as a function of the incident light intensity I_0, which is expressed in terms of power (mW). Figure 9(a) shows the case where θ_0 is set at the value close to zero ($\theta_0=-0.2°$). As I_0 is increased, I_d changes along the lower branch because the system is not exactly symmetry. At $I_0=120$ mW, the switching from the lower branch to the upper one was made by quickly changing θ_0 from the original value to a relatively large positive value and then back to the original value again. After such a procedure, the system can be set on the upper branch. As I_0 is decreased in this situation, I_T changes along the upper branch and a small jump back to the lower branch takes place at $I_0=26$ mW. The straight dashed-dotted line from the origin shows the plots of I_d in the case where the backward beam is blocked. When θ_0 is carefully adjusted to zero, we could observe the phenomenon of symmetry breaking in I_d, i.e., the random choice of its change along the upper or lower branch in

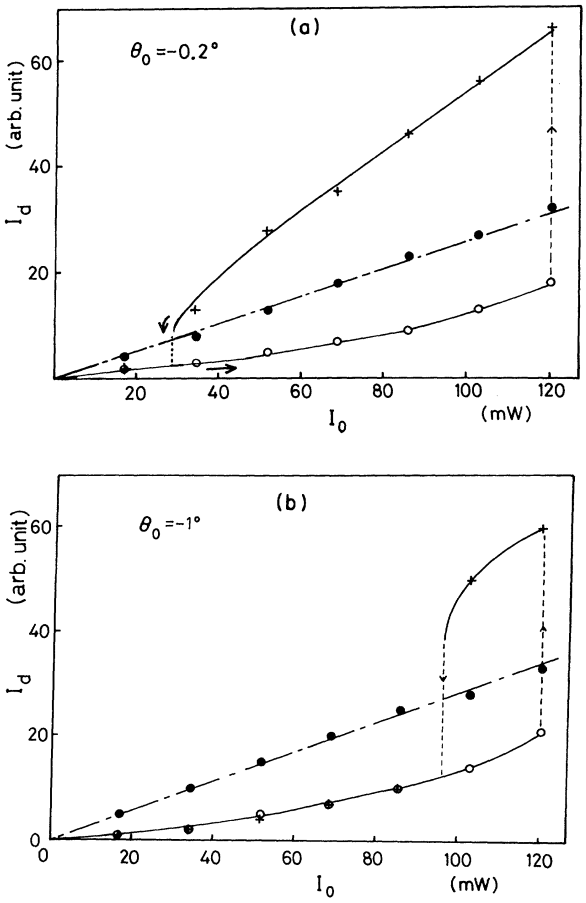

FIG. 9. Detected light intensity I_d, which is approximately proportional to $I_0\cos^2(\theta+\pi/8)$, as a function of the incident light intensity I_0 for (a) $\theta_0=-0.2°$ and (b) $\theta_0=-1°$. Black circles show the case where the backward light is blocked.

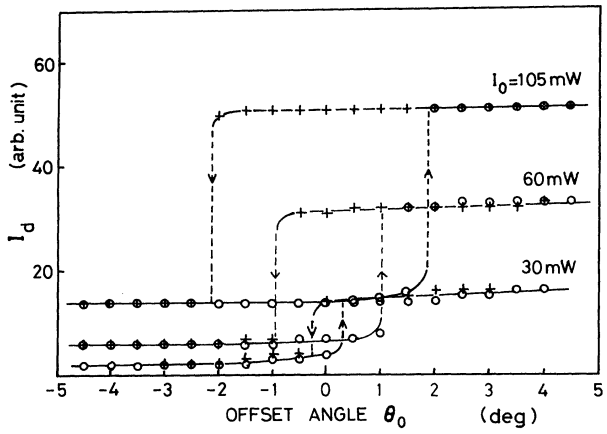

FIG. 10. Detected light intensity I_d as a function of the offset angle θ_0 for incident light intensities $I_0=30$, 60, and 105 mW.

each scan of I_d. But it was difficult to keep such a condition for a minute. Figure 9(b) shows the similar plots of I_d as a function of I_0, in the case where $\theta_0=-1°$. The switching from the lower to upper branches at $I_0=120$ mW was made by changing θ_0 as mentioned above.

In order to verify the theoretical prediction that the present system behaves with hysteresis when θ_0 is varied, we have measured I_d as a function of the offset angle θ_0, keeping I_0 constant. The results are shown in Fig. 10, for the cases where $I_0=30$, 60, and 105 mW. In Fig. 10, we clearly see a hysteresis cycle in $I_d(\theta_0)$, whose bistable region spreads out for larger values of I_0. The critical value of I_0 to obtain a hysteresis cycle was about 20 mW.

V. CONCLUSIONS AND DISCUSSIONS

In this paper we have studied a simple optically bistable system with no optical cavity and found that the behavior of this system is largely different from ordinary optical bistability reported so far. As incident light intensity I_0 is varied, the present system behaves with pitchfork bifurcation (or symmetry breaking), which is in contrast with the ordinary optical bistability with hysteresis. We have shown that the present optical bistability can well be explained in context with the cusp catastrophe similarly to the ordinary one, different features being attributable to the orthogonal cross sections of the steady-state surface of the cusp catastrophe. The constructive phenomena, hysteresis and pitchfork bifurcation, can also be regarded as the results of the first- and second-order phase transitions. In the present system, a hysteresis cycle can be obtained when one varies the offset angle θ_0 of a $\lambda/8$ plate (or a $\lambda/4$ plate in the system shown in Fig. 8). Namely, both of the first- and second-order phase transitions can be observed by varying respectively the quantities θ_0 and I_0. This is not peculiar to the present optical bistability. In a ferromagnetic material, for example, hysteresis and pitchfork bifurcation in magnetization are observed when magnetic field intensity and temperature are varied in the vicinity of the Curie point, respectively.

Theoretical study has been made on the behavior of the present system under a static field applied perpendicularly to the beam axis, and we have found that the magnetization produced spontaneously by symmetry breaking precesses around the field without any external periodic forces.

In the theoretical analysis presented in this paper, we have neglected the loss of light intensity by the absorption. Such simplification may be valid when the laser frequency is tuned on the far wing of the absorption line, as in the present experiment. When the light absorption cannot be neglected, the incident light is subjected to the circular dichroism, in addition to the rotation of polarization, which makes the polarization elliptical as it is propagated in the optically pumped medium. Numerical calculations were made in such cases, and we found that the light absorption modifies quantitatively the rotation angle θ or the magnetization m_z and critical incident light intensity I_{cr} from those presented in this paper, but it does not cause important changes in the physics involved. We found that, when the absorption loss less than about 10% for a single path, the circular dichroism is not important and the effect of light absorption can be well described by a homogeneous loss introduced in the feedback loop.

We have carried out the experiments using sodium vapor, and we have been able to obtain the evidence that the system shown in Fig. 8 behaves with symmetry breaking or pitchfork bifurcation when the offset angle θ_0 is zero. Furthermore, a hysteresis cycle has been observed when θ_0 is varied, as predicted by the theory. Experiments using the simpler system shown in Fig. 1 are now under way in our laboratory, and preliminary results show that the behavior is quite similar to that reported in this paper.

It must be pointed out that the present optical bistability has some similarities to the optical tristability, the behavior of which was theoretically studied by us[4,9] and recently observed by Cecchi *et al.*[5] and Mitchke *et al.*[10] in the experiments using sodium vapor. Similarly to the present case, the optically tristable system has a positive feedback loop for the intensity difference of two circularly polarized components of light and it exhibits symmetry breaking and self-pulsing in a static magnetic field. In the case of optical tristability, the optical feedback is done by using a Fabry-Perot cavity and differential gain is obtained by using the slope of the resonance of cavity. Three stable states observed at the same incident light intensity can be described in terms of atomic spin states: spin oriented parallel and antiparallel to the beam axis, and at random. The random spin state is unstable in the bistable region of the present case, as seen in Fig. 3(a). The important point to note is that the symmetry breaking takes place simultaneously with a jump in a doubled hysteresis cycle in the optical tristability, and such a feature can be explained in context with the butterfly catastrophe.[7]

The requirement for the laser spectrum to obtain the present optical bistability is not so severe. We have to avoid the strong absorption at the central region of the resonance line, but it is enough to tune the laser frequency roughly in a relatively wide range on the far wing. In fact, we could obtain the experimental results similar to those shown in Figs. 9 and 10, even when we used the dye laser operating on three modes with a frequency separation ~ 2 GHz. In the case of optical tristability, the laser frequency must be tuned on both wings of the atomic absorption line and of a sharp resonance of the optical cavity. So, the single-mode and highly frequency stabilized laser is required, as in the experiments of Cecchi *et al.*[5] and Mitschke *et al.*[10]

Finally it must be pointed out that the optical bistability with hysteresis can be obtained by circularly polarizing the backward light in the present system (see Appendix). Furthermore, a new type of chaos was found to occur in the present optical bistability, if the optical feedback is delayed by placing the mirror far from the cell in Fig. 1. Details are to be reported elsewhere.

APPENDIX: OPTICAL BISTABILITY WITH HYSTERESIS

We would like to show here that the optical bistability with hysteresis can be obtained by modifying slightly the optical system shown in Fig. 8. Such modification is made so that the polarization of the light fed back to the cell always becomes circular, which may easily be realized by inserting a linear polarizer between the cell and the $\lambda/4$ plate. The angle between the optical axes of the linear polarizer and the $\lambda/4$ plate is fixed at 45°. The circularly polarized backward light pumps atoms in the cell which causes the rotation of polarization of the forward light, the direction of the rotation being determined by the sense of circular polarization. Thus we see that the amplification of the rotation angle θ occurs asymmetrically in this system.

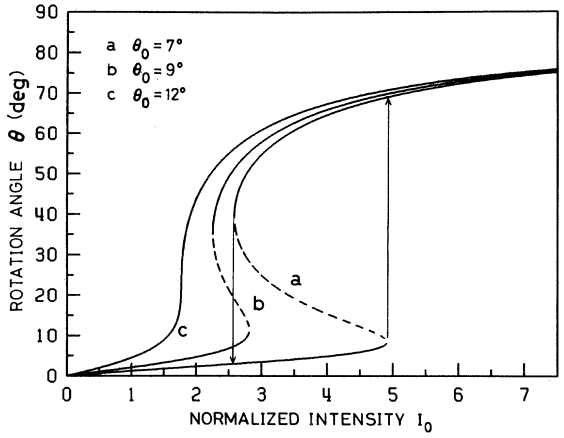

FIG. 11. Equilibrium rotation angle θ in the modified system as a function of the incident light intensity I_0 in the case where $kL = 3$. The offset angle θ_0 of the linear polarizer, defined in the literature, is varied as a parameter.

Through the analysis similar to that mentioned in Sec. II, we can easily obtain the expression giving the equilibrium rotation angle θ as

$$\theta = kL \frac{I_0 \sin^2(\theta+\theta_0)}{2+I_0[1+\sin^2(\theta+\theta_0)]}, \tag{A1}$$

where we have written again θ_0 as the angle between the direction of the incident light polarization and the direction perpendicular to the optical axis of the linear polarizer (i.e., $\theta_0 = 0$ corresponds to null transmittance of the polarizer). The absorption loss has been assumed to be negligibly small. The rotation angle θ as a function of incident light intensity I_0 in the case of $kL = 3$ is shown in Fig. 11 for three values of θ_0, where the dashed lines represent unstable equilibrium values. We see in Fig. 11 that, when θ_0 is less than a critical value ($\theta_0 = 12°$ in this case), the system exhibits the bistability with hysteresis as seen in ordinary optical bistability. In comparing with Fig. 3 we also see that the threshold value of I_0 necessary to get two stable states is three or four times higher than that in the previous case.

[1]R. Bonifacio and L. A. Lugiato, Opt. Commun. 19, 172 (1976); H. Haken, *Synergetics* (Springer-Verlag, Berlin, 1977).
[2]H. M. Gibbs, S. L. McCall, and T. N. C. Venkatesan, Phys. Rev. Lett. 36, 1135 (1976).
[3]For example, see *Optical Bistability,* edited by C. M. Bowden, M. Ciftan, and H. R. Robl (Plenum, New York, 1981).
[4]M. Kitano, T. Yabuzaki, and T. Ogawa, Phys. Rev. Lett. 46, 926 (1981).
[5]S. Cecchi, G. Guisfredi, E. Petriella, and P. Salieri, Phys. Rev. Lett. 49, 1928 (1982).
[6]A. Gozzini, C. R. Acad. Sci. (Paris) 255, 1905 (1962).
[7]R. Thom, *Structural Stability and Morphogenesis* (Benjamin, Reading, Mass., 1975); T. Poston and I. Stewart, *Catastrophe Theory and its Applications,* (Pitman, London, 1978).
[8]G. P. Agrawal and H. J. Carmichael, Phys. Rev. A 19, 2074 (1979).
[9]M. Kitano, T. Yabuzaki, and T. Ogawa, Phys. Rev. A 24, 3156 (1981).
[10]F. Mitschke, J. Mlynek, and W. Lange, Phys. Rev. Lett. 50, 1660 (1983).
[11]See, for example, A. Szöke, V. Daneu, J. Goldhar, and N. A. Kurnit, Appl. Phys. Lett. 15, 376 (1969); S. L. McCall, Appl. Phys. Lett. 32, 284 (1978); R. Bonifacio and L. A. Lugiato, Lett. Nuovo Cimento 21, 510 (1978).
[12]B. van der Pol, Proc. IRE 22, 1051 (1934).
[13]For example, see N. N. Bogoliubov and Yu. A. Mitropolsky, *Asymptotic Methods in Theory of Nonlinear Oscillations* (Fizmatgiz, Moscow, 1963).